Performance of Wireless Chemical Sensor Network With Dynamic Collaboration

Champake Mendis, Alex Skvortsov, Ajith Gunatilaka, and Shanika Karunasekera

***Abstract*— The chemical tracers dispersed by turbulent motion in the environment display rather complex and even chaotic properties. Meanwhile, chemical tracer detecting sensors with air sampling consume significant energy. Hazardous chemical releases are rare events. If all sensors in a wireless chemical sensor network (WCSN) are left in the active state continuously, it would result in significant power consumption. Therefore, dynamic sensor activation is crucial for the longevity of WCSNs. Moreover, the statistical characteristics of chemical tracers to be detected (temporal and spatial correlations, etc.) and placement of chemical sensors can also become the key parameters that influence the WCSN design and performance. In this paper, we investigate the effect of spatial correlation of a chemical tracer field, and also the effect of network topology, on the performance of a WCSN that employs an epidemiology-based dynamic sensor activation protocol. We present a simulation framework that comprises models of the spatially correlated tracer field, individual chemical sensor nodes, and the sensor network. After validating this simulation framework against an analytical model, we perform simulation experiments to evaluate the effect of spatial correlation and network topology on selected performance metrics: response time, level of sensor activation, and network scalability. Our simulations show that spatial correlation of chemical tracer field has a detrimental effect on the performance of a WCSN that uses an epidemiological activation protocol. The results also suggest that a WCSN with random network topology has poorer performance compared to one with a regular grid topology in this application.**

***Index Terms*— Correlation, energy saving, network topology, wireless chemical sensing.**

I. Introduction

WIRELESS sensor networks (WSNs) are of significant importance for defence (military operations, scenario planning, situational awareness), national security (counter-terrorism, border control), hazard management (bushfires, anthropogenic catastrophes), ecological monitoring (air pollution, wildlife, water quality) and some industrial applications (control of technological processes). Some recent initiatives (for example, by USA Department of Homeland Security, [1]) aimed at developing tiny chemical sensors that can be embedded in a conventional mobile phone make feasible the construction of wireless chemical sensor networks (WCSNs) with massive numbers (thousands or even millions) of nodes. The purpose of such WCSNs is to detect, identify, and characterise the dynamic chemical threats associated with tracer fields, such as aerosol, gas, moisture, etc., by using the advantages of collaborative performance of sensors over those of individual nodes. As the number of sensors increases, however, the design and management of such systems become challenging tasks that require mathematical modeling, computer simulation, and parameter optimization.

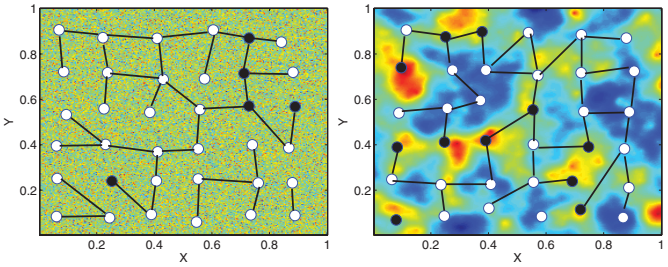

Fig. 1. Graphical illustration of WCSNs operating in simulated chemical tracer fields that are: (a) spatially noncorrelated and (b) spatially correlated. The tracer fields are depicted as 2-D xy-planes, with different colors representing different tracer concentrations. The empty white circles represent active sensors, and the filled black circles represent inactive sensors.

It is well known that chemical tracers (throughout this paper, we use the terms 'chemical tracers', 'chemical contamination' and 'threat' interchangeably) dispersed by turbulent motion in the environment display rather complex and even chaotic properties (so-called phenomenon of scalar turbulence [2]). The underlying complexity of the tracer field imposes additional challenges on the WCSN architecture. Moreover, the statistical characteristics of chemical tracers to be detected (temporal and spatial correlations, etc.) can become the key parameters that influence the WCSN design and performance. In application to other types of WSNs (sonar, radio, optical, etc.), the studies of these effects have a long history, and they are well documented. The current study deals with the correlation effects that are specific to a tracer advected by turbulent flow in the ambient environment (i.e., low velocity of tracer propagation, intermittent distributions, power-law tails of probability density function (PDF)). In this context, we estimate the contribution of spatial correlations to the positive

Manuscript received February 20, 2012; accepted April 17, 2012. Date of publication May 8, 2012; date of current version June 6, 2012. The associate editor coordinating the review of this paper and approving it for publication was Dr. M. Nurul Abedin.

C. Mendis and S. Karunasekera are with the Department of Computing and Information Systems, University of Melbourne, Melbourne 3053, Australia (e-mail: mendisc@csse.unimelb.edu.au; karus@unimelb.edu.au).

A. Skvortsov and A. Gunatilaka are with the Human Protection and Performance Division, Defence Science and Technology Organization, Fishermans Bend 3207, Australia (e-mail: alex.skvortsov@dsto.defence.gov.au; ajith.gunatilaka@dsto.defence.gov.au).

Color versions of one or more of the figures in this paper are available online at http://ieeexplore.ieee.org.

Digital Object Identifier 10.1109/JSEN.2012.2198349

detection of hazardous threats by simulating different types of WCSNs in tracer fields with different correlation structures (short and long correlated; see Fig. 1(a) and Fig. 1(b)). We also briefly examine the effect of network topology (node connectivity) on the WCSN's performance.

Apart from the aforementioned characteristics of the underlying chemical tracer field, chemical sensors themselves also have unique characteristics that differentiate them from other types of sensors that are typically used in wireless sensor networks. Particularly, unlike other types of sensors, such as optical or acoustic sensors, typical chemical sensors with air sampling consume significant energy for sensing activity compared to what is consumed for communication. Because hazardous chemical releases are rare events, if all sensors in a WCSN are left in the active state continuously, it would result in significant power consumption. Therefore, dynamic sensor activation is crucial for the longevity of WCSNs. Dynamic sensor activation for chemical sensor networks using an 'epidemiological' sensor activation protocol has been proposed in previous work of [3]. In this protocol, the information on tracer presence is spread amongst WCSN nodes similar to a disease epidemic in a community. This protocol provides a well developed analytical framework, rich physics-based analogies (epidemiology, percolation, network models, etc.), and simple computer implementation in the form of coupled ordinary differential equations (ODE). The significant simplifications associated with employing 'epidemiological' approach enables the conducting of some optimization studies which would be difficult (if not unfeasible) to perform by any other way. Several performance aspects such as the effect of topology [4], [5] and energy consumption [6] of WCSNs with epidemiological sensor activation have been studied previously assuming the underlying tracer fields to be spatially uncorrelated.

In this paper, we present the findings of a simulation study performed to evaluate the performance of a WCSN with an epidemiology-based sensor activation protocol in the presence of non-correlated and correlated chemical tracer fields. Specifically, we make the following contributions.

1) We evaluate the effect of spatial correlation of tracer fields on some performance metrics of the WCSN (namely, fraction of active sensors, response time, interaction rate, and network scalability).
2) We assess the impact of two sensor network topologies (namely, regular grid and uniform random grid) on the same three metrics (i.e., fraction of active sensors, response time, interaction rate, and network scalability).

II. Related Work

The effect of correlation structure of the environment on WSN architecture and its operational protocol has been actively investigated, and the results are well-documented in the literature (see [7], [8], and [9] and references therein). Many of these studies are concerned with data redundancy, aggregation, and energy consumption of WSNs. The investigation of these considerations in WCSNs has been started only recently; the research study by Ma *et al.* [10] is one such instance. The reason for this relative lack of studies of WCSNs is two-fold. Firstly, a reliable chemical sensor is a complex technical device (which often contains an air-sampling unit), so development of WCSNs with an appreciable number of sensors has been considered as impractical until recently. Secondly, high fidelity statistical modeling of tracer distribution in turbulent flow (consistent with the results of the theory of turbulent mixing and dispersion) is a challenging task and still an area of active research [2]. A full-scale implementation of such models still requires expert knowledge in computational fluid dynamics and advanced computer resources. As for simplified models, there are surprisingly few that can provide consistent temporal and spatial statistics, and this is still an area of active research as well [11]–[13].

Some of the first examples of simulating a WCSN operating in a turbulent environment are presented by Dekker and Skvortsov [4] and then by Skvortsov *et al.* in [3]. There, the authors proposed a simple mathematical model for WCSN with an epidemiology-based activation protocol and a turbulent chemical tracer environment modeled by a random time series. Dekker and Skvortsov [4] investigated the effect of network topology on WCSN performance. Of six networks examined, they found a square grid and a network with short range random links to have the best performance. Skvortsov *et al.* [3] derived analytical expressions that relate the parameters of the network (e.g., number of sensors, their density, sensing time) with the parameters of network performance (probability of detection, response time of network) and the parameters of the external challenge (the chemical pollutant and environment). In physical implementations, Vito *et al.* [14] present polymer-carbon chemical sensors with inbuilt intelligence for distributed sensing and censoring transmission to reduce power consumption. This substantiates the feasibility of using an epidemiology-based protocol in intelligent sensor activation. While the analogy between epidemiology and a wireless communication operational protocol has become a topic of intensive sensor network research and development activity in the recent past (see [15], [16] and references therein), due to aforementioned reasons, there is a notable lack of studies focussed on WCSN.

III. System Modeling and Simulation

For the purpose of system simulation, we developed a simulation framework comprising three independent models representing the environment (the spatiotemporal realisation of the concentration field of the chemical tracers caused by turbulent mixing), an individual chemical sensor node, and the whole WCSN. This modular design of the simulation framework allows gradual improvements in any of these models. We validated our simulation model by comparing simulated results against an analytical model. The three component models of our simulation framework as well as the analytical model are discussed below.

A. Model of Environment

We consider a chemical tracer field covering a square region of side length L and area S ($S = L^2$). We assume that all

sensor nodes of our system are deployed at the same height; so, we are interested in 2D tracer concentrations.

Our modeling framework allows generation of two dimensional concentration slices for a given functional form of PDF, $p(c)$; for details see [17]. The chemical tracer field is modeled as a sequence of time-varying random data slices which mimics the turbulent fluctuations of concentration at each point in the 2D xy-plane of interest where the sensor nodes are deployed. Because the main focus in this study is on the effect of spatial correlation of chemical tracers on WCSN performance, in our simulations we use concentration slices that have spatial correlation but are temporally uncorrelated. This mimics the case when the characteristic time of the turbulent fluctuations of tracers is greater than the typical sampling time of the chemical sensor (usually, a few seconds to tens of seconds).

As a benchmark for comparing the effect of spatial correlation on WCSN performance, we use the case where the tracer is spatially non-correlated. To simulate non-correlated tracer fields, we use the simple model of a clipped Gaussian distribution and draw random data that represent uncorrelated concentration fluctuations. For simulating the spatially correlated concentration fields, we first generate non-correlated concentration data as above and filter the data using a two-dimensional exponential filter. The amount of spatial correlation is controlled by changing the sharpness of the exponential filter kernel. The mean concentration of the tracer field is C_0 while the variance of the tracer distribution depends on the level of spatial correlation. We normalise the correlation radius R_{corr} by tracer field size L and express the degree of correlation by a non-dimensional parameter ω as follows:

$$\omega = \frac{R_{corr}}{L}. \tag{1}$$

Low values of ω correspond to underlying tracer fields with low spatial correlations and vice versa; the non-correlated case, in which the correlation radius R_{corr} approaches zero, corresponds to $\omega = 0$.

B. Model of a Chemical Sensor Node

In an ion mobility spectroscopy based chemical sensor, a set volume of air is drawn first. The air molecules ionized by a weak radioactive source, when sent through an electric field, are accelerated. With different arrival times of different ion types at the ion collector, bar readings can be created and classified by agent type [18]. In this study, we adopt a simple binary (or 'threshold') model of a sensor with air sampling. In this model, the sensor reading V is given by

$$V = \begin{cases} 1, & C \geq C_* \\ 0, & C < C_* \end{cases} \tag{2}$$

where C is the tracer concentration at a sensor location, and C_* is the chemical tracer detection threshold, an internal characteristic of sensors, unrelated to the mean concentration C_0. The parameter C_* enables continuous estimation of probability of the tracer concentration to exceed sensor threshold: $p = 1 - F(C_*)$, where $F(.)$ the cumulative distribution function of tracer concentration for a given form of $p(c)$. A sensor is also characterised by its detection period τ_*; i.e., the time taken for the sensor to sample the air and make a determination whether a tracer concentration above its detection threshold is present.

We consider each sensor node to be capable of communicating in an omni-directional fashion with its neighboring nodes that are within a communication range r_*. By normalising the communication radius r_* by tracer field size L, we express it as a non-dimensional parameter δ as follows:

$$\delta = \frac{r_*}{L}. \tag{3}$$

We also define another non-dimensional parameter ϵ to describe the correlation of a chemical tracer field as a factor of communication radius r_* as follows:

$$\epsilon = \frac{R_{corr}}{r_*}. \tag{4}$$

When ϵ is less than one, communication occurs beyond a correlated tracer blob.

C. Model of Chemical Sensor Network

We consider a WCSN consisting of N identical chemical sensor nodes and covering the full area of the chemical tracer field. Each sensor node can be in one of two states: $passive$ or $active$. Apart from the controlled activation of a small number of sensor nodes (four in our simulations) at the start of each simulation for bootstrapping the WCSN, a passive sensor can become active only when it receives a message from an active neighbor. If an active sensor detects a chemical tracer concentration above the detection threshold, it remains active and broadcasts an 'activation' message to its neighbors that are within its broadcast range r_* (We assume ideal, error-free communication and avoid considerations of interferences, contentions, etc.); otherwise, it becomes passive and remains so until 'woken up' again by an active neighbor. In other words, only those active sensors that make a detection are retained in the active state. This constitutes a single cycle or a time step in the WCSN life cycle. In the present study, we consider two WCSN topologies: regular grid and uniform random grid.

D. Analytical Model

The behaviour of the WCSN described in the previous section is similar to the epidemic SIS (susceptible-infected-susceptible) model in [19], in which an individual in a community is in one of two states: susceptible to an identified disease; or infected by the disease. In this context, the passive sensors are analogous to susceptible individuals, and active sensors are analogous to infected individuals. For simplicity, we accept all inactive or passive sensors as susceptible unlike in a real world scenario, where susceptible individuals are the ones who are in contact with the infected individuals. Based on this intimate analogy with the process of an epidemic, an analytical model in the form of a closed system of ODE

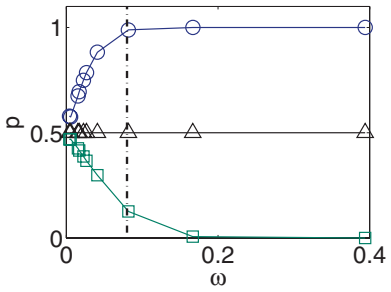

Fig. 2. Variation of probability of detection (p) of a sensor as a function of the nondimensional correlation parameter (ω), defined in (1), for different value ranges of the sensor detection threshold (C_*). $C_* < C_0$ ($\circ$), $C_* = C_0$ ($\triangle$), and $C_* > C_0$ ($\square$). C_0 is the mean concentration of the chemical tracer field. The dashed line corresponds to $\omega = 0.08$.

can be derived to describe the dynamics of the WCSN [3]

$$\frac{dN_+}{dt} = \alpha N_+ N_- - \frac{N_+}{\tau_*}, \tag{5}$$

$$\frac{dN_-}{dt} = -\alpha N_+ N_- + \frac{N_+}{\tau_*} \tag{6}$$

where N_+ and N_- denote the number of active and passive sensors, respectively. The population size (i.e., the total number of sensors) is conserved, that is $N_+ + N_- = N = const$. The non-linear terms on the RHS of Eq. (5) and Eq. (6) are responsible for the interaction between individuals (i.e., sensors), with the parameter α being a measure of this interaction. Based on the epidemiological analogy, the following analytical expression for the interaction parameter α is proposed by Skvortsov *et al.* [3]:

$$\alpha = G\frac{\pi r_*^2}{\tau_* S} p \tag{7}$$

where S is the square area covered by a WCSN, and G is the calibration factor, being of order unity, and parameter p, as above, is expressed in terms of the cumulative distribution function: $p = 1 - F(C_*)$; parameter p is a function of the sensor detection threshold C_* and the non-dimensional parameter ω, defined in Eq. (1). In the synthetic chemical tracer model [20], we use, as Figure 2 shows the influence of C_* on the probability of detection p of chemical tracers by a sensor for fields with different correlation structures.

It can be seen that when $C_* < C_0$, p increases with ω, and when $C_* > C_0$, p decreases with ω; when $C_* = C_0$, p is independent of ω, and it is an ideal value to keep the p value at a constant level for experimentation.

The SIS protocol, represented by Eq. (5) and Eq. (6), can be easily treated analytically and allows us to model a variety of responses and perform various optimization studies. This analytical form also provides us with a valuable performance check for our simulations. Skvortsov *et al.* [3] found the analytical solution of the system to be given by

$$z(t) = \frac{z_0}{(1 - z_0)\exp(-bt) + z_0} \tag{8}$$

where $z(t) = N_+/N$, $z_0 = z(0)$, and

$$b = \alpha N - \frac{1}{\tau_*}. \tag{9}$$

It can be seen that $z(t)$ increases only if $b > 0$ (otherwise $z(t) \to 0$). This condition corresponds to an *information epidemic* (IE) [3], [21] and can be re-written as

$$\alpha N \tau_* > 1 \tag{10}$$

or by substituting from Eq. 7, expressed as

$$GNp\left(\frac{\pi r_*^2}{S}\right) > 1. \tag{11}$$

For given values of other parameters, this condition can always be met by increasing the number of sensors N. From our computer simulations, we can estimate the fraction of active sensors as $z(t) = \frac{N_+}{N} = 1 - \theta$. Then the interaction rate α can be computed from:

$$\alpha = \frac{1}{\theta \tau_* N}. \tag{12}$$

IV. Validation of WCSN Model

To validate our WCSN simulation model against the analytical model of Eq. (8), simulation experiments were performed using WCSNs of both the regular grid topology and the uniform random topology, with non-correlated ($\omega = 0$) and correlated ($\omega = 0.02$ to 0.39) chemical tracer fields, we show results for ($\omega = 0.08$) here, as it is considered as an ideal value with diverse properties as shown in Figure 2. The following simulation parameter values were used in these validation experiments: $N = 400$ sensors, $L = 250$ units, the sensor detection threshold was held at $C_* = C_0$ and $r_* = 20$ units (equivalently, $\delta = 0.08$ in non-dimensional form). All results in the paper will be presented in terms of non-dimensional parameters to make it possible to scale the results without being tied to particular measurement units.

Figure 3 shows the results of validation experiments for the two network topologies in the presence of non-correlated and correlated tracer fields; in this figure, elapsed time t is shown as a non-dimensional parameter $\kappa = t/\tau_*$. The time evolution of the fraction of active sensors (N_+/N) obtained from simulations show sigmoidal patterns similar to that obtained by Eq. (8). We first empirically estimated b by fitting curves of the analytical form of Eq. (8) to simulated data and estimated the corresponding calibration constant G using Eq. (7) and Eq. (9). For all cases, the calibration parameter G was found to be of the order of unity.

As shown in Figure 3, the good agreement between analytical and simulated results validates our simulation model. The experiments to evaluate the performance are presented in the Section V.

V. Numerical Results

In this section, we describe and present the results of three numerical experiments performed using our simulation framework to evaluate the performance of WCSNs. In these experiments, simulations were carried out using WCSN models of both regular grid and uniform random topologies in the presence of simulated tracer fields with several different levels of spatial correlation, including the non-correlated limit.

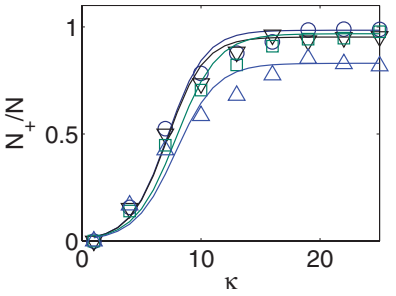

Fig. 3. Comparison of the analytical model defined (8) against the simulation models of a WCSN: $\omega = 0.00$, regular grid topology ($\circ$), $\omega = 0.00$, random topology ($\triangledown$), $\omega = 0.08$, regular grid topology ($\square$), and $\omega = 0.08$, random topology ($\triangle$). The solid lines show the analytically fitted curves. Here, N_+ is the number active sensors, and N is the total number of sensors in the WCSN. $\kappa = t/\tau_*$ is the normalized time where τ_* is the detection period of a sensor.

A. Experiment 1: Effect on Sensor Activation

The first experiment was carried out to determine the effect of network topology and chemical tracer field correlation on the sensor activation of WCSN. A fraction of active sensors N_+ at saturation state is a measure of the network (positive) response to the event of chemical contamination. In this experiment, WCSNs of both regular grid and uniform random topologies were simulated in the presence of a simulated chemical tracer field with no spatial correlation ($\omega = 0$) and one with correlation ($\omega = 0.08$). The number of sensors was again set at $N = 400$, and the sensor detection threshold was held at $C_* = C_0$. Simulations were performed for several values of communication radius r_* (or equivalently, the non-dimensional parameter δ); specifically, the following δ values were used for plotting: $\delta = 0.052$, $\delta = 0.056$, $\delta = 0.080$, $\delta = 0.160$, and $\delta = 0.480$. Each scenario was simulated 25 times, varying the bootstrapping sensors in the case of the regular grid sensor network and varying the sensor locations themselves in the case of the random sensor network. Figures 4(a) and 4(b) show ensemble averaged results obtained for regular grid and Figures 4(c) and 4(d) show those for random WCSN.

We see a rise in the saturation level of the IE and a decrease of response time τ when the communication radius r_* (or δ) is increased or ϵ is decreased. We see that some low values of δ do not support an IE; i.e., the IE 'dies out', as the condition for an IE is not satisfied in these cases. In a regular grid topology, sensors are well distributed and capable to bear the drastic changes in the environment, where in the case of random topology sensors may be not within a chemical tracer concentration for collaborative activation and IE to continue. We can say that blobs instead well dispersed chemical tracers of high concentration, insufficient sensor connectivity tend to hinder the IE process. We observe that results are in compliance with Eq. (8), however with different values for calibration constant G.

B. Experiment 2: Empirical Modeling of Interaction Rate

The aim of the second experiment was to derive an empirical model for the interaction rate α for a WCSN of regular grid topology in a correlated chemical environment, based on our numerical simulation data. The experiment was performed by varying r_* (or δ) over a wide range. (from very small values to a radius large enough to communicate from one corner to the other in the field covered by WCSN). The sensor detection threshold was fixed at $C_* = C_0$, side length $L = 500$ units and calibration constant $G = 0.13$. In this, we used the best performing WCSN of regular grid topology in the chemical tracer field with spatial correlation.

As r_* was incremented, the interaction rate α was computed analytically (using Eq. (7)) and from simulation results (based on Eq. (12)). We denote the analytical value of α by α_a and the simulated value by α_s. Figure 5 shows the comparison of α_s and α_a. As r_* is increased, the interaction rate estimated from simulations α_s increases gradually and reaches a saturation value, which we denote by α^*.

We did not find notable differences of α^* with different deployed areas, network topologies, and correlation structures [22]. However, when the process was repeated using a different number of sensors, the saturation value α^* was found to change. Therefore, we repeated the simulations for a range of N (all square numbers between 400 and 3600) and obtained the simulated and analytical interaction rates.

Figure 5 shows that Eq. (7) consistently underestimates the value of α for lower r_* and overestimates for higher r_*. But the overall estimate is within an acceptable range, and we can write a simple but universal estimate for the interaction parameter for a given N as: $\alpha_a \leq \alpha \leq \alpha^*$, where α^* is the saturation level. We believe this discrepancy between the simulated and analytical values of the interaction rate is due to the effect of double counting of activation messages in overlapping areas of activation in the sensor network [3]. We can expect a better match by varying the calibration parameter G. As a better alternative, we derive a robust empirical model for the interaction rate α. In compliance with our intuitive assumption, we see that the interaction rate α and saturation state α^* decrease when the number of sensors N increases. Based on the intuitive assumption that α^* and N have a power law relationship, we can write

$$\alpha^* \propto N^{\beta} \tag{13}$$

where the power law exponent β is a fitting parameter. From the plot of α^* vs. N in log-log scale, shown in Figure 6, we estimate that $\beta \approx -1$.

Next, for different values of N, we plot α, normalised by the saturation value α^*, as a function of the normalised communication radius δ, as shown in Figure 7. From this figure, we see that the curves corresponding to all values of N collapse into a single universal curve which fits a function of the form

$$\frac{\alpha}{\alpha^*} = 1 - \exp(-a\delta). \tag{14}$$

The fitting parameter in Eq. (14) is estimated to be: $a = 5.8$.

C. Experiment 3: Scaling Laws of WCSN Performance

The final experiment was performed to ascertain the scalability of the WCSN. The scalability of any sensor system is a parameter that usually describes the system performance as

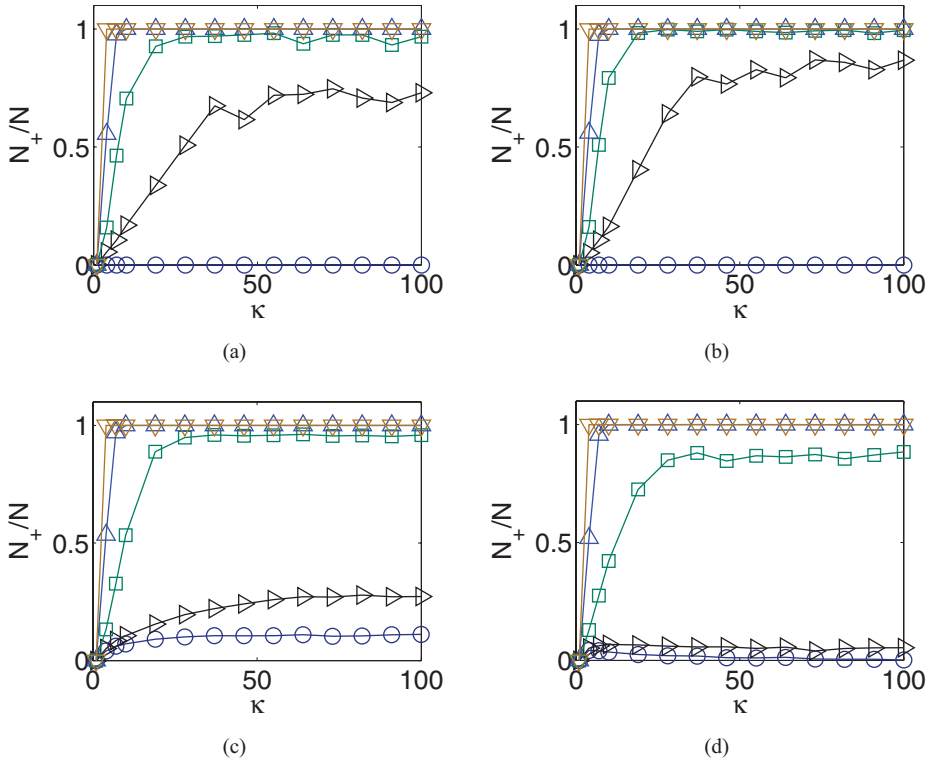

Fig. 4. Effect of communication range (r_*) on the onset of IEs (N_+/N) in a WCSN: (a) regular grid topology in noncorrelated tracer field, (b) regular grid topology in correlated tracer field, (c) random topology in noncorrelated tracer field, and (d) random topology in correlated tracer field. The range of values used for the nondimensional communication radius parameter δ, defined in (3), are: $\delta = 0.052$ ($\circ$), $\delta = 0.056$ ($\triangleright$), $\delta = 0.080$ ($\square$), $\delta = 0.160$ ($\triangle$), and $\delta = 0.480$ ($\triangledown$). $\kappa = t/\tau_*$ is the normalized time where τ_* is the detection period of a sensor.

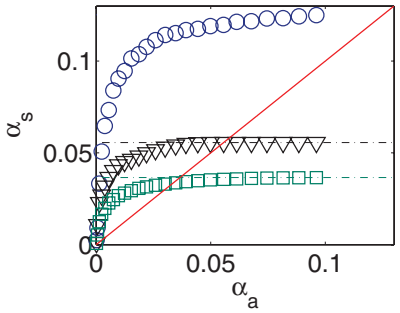

Fig. 5. Comparison of simulated [α_s from (7)] and analytical [α_a from (12)] values of interaction rate α in a WCSN with regular grid topology in the presence of a correlated tracer field, with the number of sensors equal to: $N = 400$ ($\circ$), $N = 900$ ($\triangledown$), $N = 1369$ ($\square$). Dash dotted lines show the saturation levels corresponding to the scenarios. The solid line shows the expected outcome if simulated and analytical values are in perfect agreement.

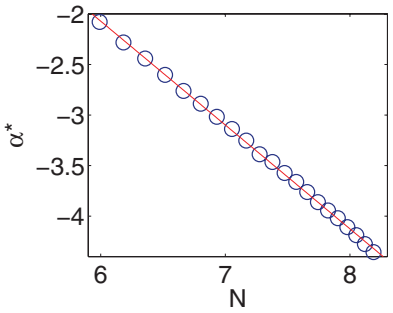

Fig. 6. Saturation value of interaction rate (α^*) as a function of the number of sensors (N), plotted in log-log scale. The best linear fit is shown as a solid line.

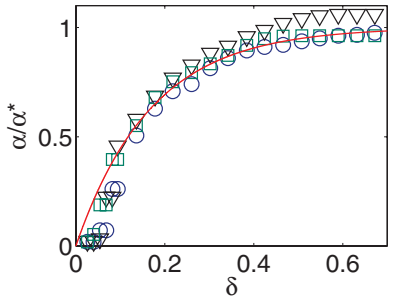

Fig. 7. Interaction rate (α), normalized by its saturation value (α^*), as a function of the nondimensional communication radius parameter (δ), defined in (3), for a WCSN operating in a correlated tracer field and having a regular grid topology with different number of sensors: $N = 400$ ($\circ$), $N = 900$ ($\triangledown$), and $N = 1369$ ($\square$). The solid line shows a curve fitted by varying a of (14).

a function of the number of deployed sensors. This is one of the important parameters that is used to shape the network architecture. The proposed framework enables straightforward derivation of the scalability factor for the WCSN.

Let us characterise the WCSN performance as a ratio $\Psi = \sigma_{N_+}/\mu_{N_+} \propto \Xi^q$, where μ_{N_+} is the time-averaged mean of N_+ (i.e., around the saturation level), and σ_{N_+} is the time-averaged fluctuations of N_+ and $\Xi = 1/N$. The scalability properties of the WCSN can then be characterised by the power exponent q in the functional relationship $\Psi \sim \Xi^q$ where N is the number of sensors, and the case $q \geq 0$ should be held for any sustainable network architecture.

In this experiment, we varied the number of sensors N while keeping the normalised communication radius fixed

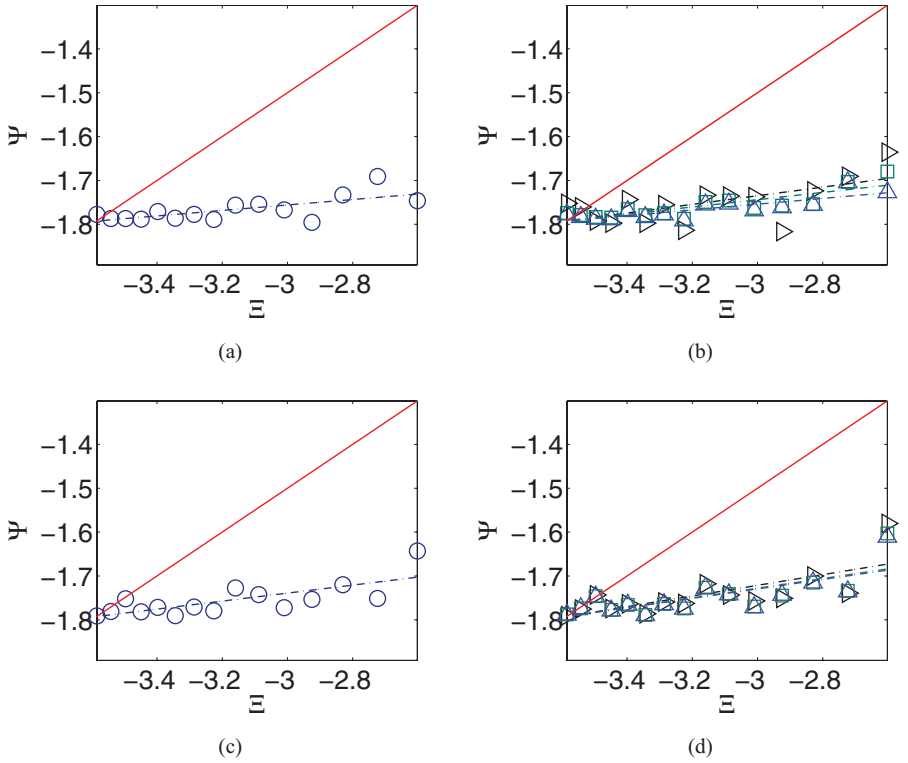

Fig. 8. Relative fluctuations $\Psi = \sigma_{N_+}/\mu_{N_+} \propto \Xi^q$, where $\Xi = 1/N$, plotted in log-log scale for a WCSN: (a) regular grid topology in noncorrelated tracer field, (b) regular grid topology in correlated tracer field, (c) random topology in noncorrelated tracer field, and (d) random topology in correlated tracer field. The correlation of tracer fields is characterized by $\epsilon = 0.00$ (○), $\epsilon = 1.02$ (▷), $\epsilon = 0.33$ (□), and $\epsilon = 0.28$ (△). The dash dotted lines show lines fitted by varying q. The solid lines show the outcome for a WCSN of independent sensors with Gaussian noise.

at $\delta = 0.08$ and sensor detection threshold at $C_* = C_0$. The lower bound of N was chosen as the minimum number of sensors that can propel an IE, and the upper bound was chosen subject to computer memory constraints. Simulations for this experiment were performed for networks with regular grid and random network topologies, operating in tracer fields with various levels of spatial correlation.

Plots of relative fluctuations Ψ versus Ξ, the reciprocal of the number of sensor nodes, are shown in Figures 8(a) and 8(b) for the regular grid WCSN and in Figures 8(c) and (d) for the random WCSN. For comparison, each figure also shows asymptotes in red which correspond to a scalability factor $q = 1/2$ that holds for any system of independent sensors with Gaussian noise, following from the standard estimate $\Psi \sim \sigma_{D_+}/\mu_{N_+} \sim \Xi^{1/2}$.

From these plots, we can see an asymptotic relationship of ϵ and fluctuations of N_+, demonstrating a power law behaviour, and we estimate the scalability factor q to be: $q \approx 0.1$ in all scenarios considered. We can see that the scalability of the WCSN with epidemic protocol follows correct trends (i.e., $q > 0$). Depending on a particular operational scenario, some other parameters (energy conservation, reliability of detection, activation time, budget, etc.) may become more important and would favour a particular technical solution.

VI. Conclusion

In this paper, we investigated the effect of spatial correlation of a chemical tracer field, and also the effect of network topology, on the detection of a chemical threat using a WCSN. To perform this study, we constructed a simple integrated simulation framework comprising models of the environment, individual chemical sensors, and the sensor network. Our WCSN used an epidemiology-based sensor activation protocol. Using a 'bio-inspired' analytical model for a WCSN, initially introduced by Skvortsov *et al.* [3], we verified the simulation framework for WCSNs of regular grid and uniform random network topologies operating in the presence of simulated tracer fields with and without spatial correlation. Based on simulation results, we evaluated some important performance metrics (namely, detection time, fraction of active sensors, sensor interaction rate, and scalability factor).

In general, we found random network topology and spatial correlation of tracer distribution (which is typical for most operational scenarios) to have a negative effect on the performance of a WCSN with the 'epidemiology' based sensor activation protocol. It manifests in longer network detection time and a lower fraction of active sensors, which is detrimental to good detectability [23]. This result contrasts with what is observed more commonly in other types of WSNs. The other possible reason for the different behaviour in our simulation is the nature of the chemical tracer field itself, involving blobs of high concentration, which is a direct consequence of mass conservation. This structure is different to the more coherent variations typical of phenomena such as optical or acoustic fields.

The work reported in this paper may be extended in future in several directions by making gradual improvements to one or more of the model components of the simulation framework: model of the environment, model of chemical sensor, and the

model of the WCSN to make each model more realistic. We will report these extensions in separate publications.

REFERENCES

[1] *Crowdsourcing: Cell Phones that Protect Against Deadly Chemicals?* (2010, Apr.) [Online]. Available: http://www.sciencedaily.com/releases/2010/04/100409162722.htm

[2] B. I. Shraiman and E. D. Siggia, "Scalar turbulence," *Nature*, vol. 405, no. 6787, pp. 639–646, 2000.

[3] A. Skvortsov, B. Ristic, and M. Morelande, "Networks of chemical sensors: A simple mathematical model for optimisation study," in *Proc. 5th Int. Conf. Intell. Sensors, Sensor Netw. Inf. Process.*, Dec. 2009, pp. 385–390.

[4] A. Dekker and A. Skvortsov, "Topological issues in sensor networks," in *Proc. Int. Congr. Model. Simul.*, Cairns, Australia, Jul. 2009, pp. 952–958.

[5] S. Karunasekera, A. Skvortsov, A. Gunatilaka, and C. Mendis, "A decentralized dynamic sensor activation protocol for chemical sensor networks," in *Proc. 9th IEEE Int. Symp. Netw. Comput. Appl.*, Jul. 2010, pp. 218–223.

[6] S. Karunasekera, A. Skvortsov, and A. Gunatilaka, "Minimizing the operational cost of chemical sensor networks," in *Proc. 6th Int. Conf. Intell. Sensors, Sensor Netw. Inf. Process.*, Dec. 2010, pp. 37–42.

[7] Y. Sung, H. Poor, and H. Yu, "How much information can one get from a wireless ad hoc sensor network over a correlated random field?" *IEEE Trans. Inf. Theory*, vol. 55, no. 6, pp. 2827–2847, Jun. 2009.

[8] M. C. Vuran, O. B. Akan, and I. F. Akyildiz, "Spatio-temporal correlation: Theory and applications for wireless sensor networks," *Comput. Netw.*, vol. 45, no. 3, pp. 245–259, 2004.

[9] L. Zhang, X. Wang, and S. Li, "A routing algorithm based on clusters and balanced use of energy for wireless sensor networks," *J. Control Theory Appl.*, vol. 8, no. 1, pp. 81–85, 2010.

[10] Y. Ma, Y. Guo, X. Tian, and M. Ghanem, "Distributed clustering-based aggregation algorithm for spatial correlated sensor networks," *IEEE Sensors J.*, vol. 11, no. 3, pp. 641–648, Mar. 2011.

[11] V. Bisignanesi and M. Borgas, "Models for integrated pest management with chemicals in atmospheric surface layers," *Ecol. Model.*, vol. 201, no. 1, pp. 2–10, 2007.

[12] S. Basu, E. Foufoula-Georgiou, and F. Porté-Agel, "Synthetic turbulence, fractal interpolation, and large-eddy simulation," *Phys. Rev. E*, vol. 70, no. 2, pp. 026310-1–026310-11, Aug. 2004.

[13] C. Rosales and C. Meneveau, "A minimal multiscle Langragian map approach to syntehsize non-Gaussian turbulent vector fields," *Phys. Fluids*, vol. 18, no. 7, pp. 075104-1–075104-14, 2006.

[14] S. De Vito, P. Di Palma, C. Ambrosino, E. Massera, G. Burrasca, M. Miglietta, and G. Di Francia, "Wireless sensor networks for distributed chemical sensing: Addressing power consumption limits with on-board intelligence," *IEEE Sensors J.*, vol. 11, no. 4, pp. 947–955, Apr. 2011.

[15] S. Eubank, V. A. Kumar, and M. Marathe, "Epidemiology and wireless communication: Tight analogy or loose metaphor?" in *Bio-Inspired Computing and Communication* (Lecture Notes in Computer Science), vol. 5151, P. Liò, E. Yoneki, J. Crowcroft, and D. Verma, Eds. Berlin, Germany: Springer-Verlag, 2008, pp. 91–104.

[16] A. Khelil, C. Becker, J. Tian, and K. Rothermel, "An epidemic model for information diffusion in MANETs," in *Proc. 5th ACM Int. Workshop Model. Anal. Simul. Wireless Mobile Syst.*, 2002, pp. 54–60.

[17] A. Gunatilaka, B. Ristic, A. Skvortsov, and M. Morelande, "Parameter estimation of a continuous chemical plume source," in *Proc. 11th Int. Conf. Inf. Fusion*, Jun.–Jul. 2008, pp. 1–8.

[18] P. Robins, V. Rapley, and P. Thomas, "A probabilistic chemical sensor model for data fusion," in *Proc. 7th Int. Conf. Inf. Fusion*, 2005, pp. 1116–1122.

[19] J. D. Murray, *Mathematical Biology*, vol. 1. New York: Springer-Verlag, 2002.

[20] C. Mendis, A. Gunatilaka, B. Ristic, S. Karunasekera, and A. Skvortsov, "Experimental verification of evolutionary estimation algorithms for radioactive source localisation," in *Proc. 5th Int. Conf. Intell. Sensors, Sensor Netw. Inf. Process.*, Dec. 2009, pp. 151–156.

[21] A. Skvortsov and B. Ristic, "Modelling and performance analysis of a network of chemical sensors with dynamic collaboration," *CoRR*, vol. 2012, pp. 1–21, Nov. 2011.

[22] C. Mendis, A. Gunatilaka, A. Skvortsov, and S. Karunasekera, "The effect of correlation of chemical tracers on chemical sensor network performance," in *Proc. 6th Int. Conf. Intell. Sensors, Sensor Netw. Inf. Process.*, Dec. 2010, pp. 103–108.

[23] F. Zhao and L. Guibas, *Wireless Sensor Networks: An Information Processing Approach*. San Francisco, CA: Morgan Kaufmann, 2004.

Champake Mendis received the B.Sc. (Hons.) degree in computer science from the School of Computing, University of Colombo, Colombo, Sri Lanka, and the M.Eng.Sc. degree (first class) in mechatronics from the University of Melbourne, Melbourne, Australia.

He has been with the Department of Computing and Information Systems, University of Melbourne, Melbourne, since 2009. His current research interests include the areas of wireless sensor networks and bio-inspired algorithms for data fusion, with emphasis on numerical modeling, simulation, and performance analysis.

Alex Skvortov received the Ph.D. degree in applied mathematics (fluid dynamics) from the Moscow University of Technology, Moscow, Russia.

He was involved in research and development projects on ocean acoustics and vortex noise modeling. He was an IT Consultant in the areas of mathematical modeling, data warehousing, and decision support systems. He joined the Defense Science and Technology Organization, Fishermans Bend, Australia, in 2005. He is currently a Science Team Leader with the Modeling, Analysis, and Physical Sciences Group, Human Protection and Performance Division, Defence Science and Technology Organization.

Ajith Gunatilaka received the B.Sc. (engineering) (Hons.) degree in electronics and telecommunication engineering from the University of Moratuwa, Moratuwa, Sri Lanka, in 1990, and the Ph.D. degree in electrical engineering from Ohio State University, Columbus, in 2000.

He has been a Defense Scientist with the Human Protection and Performance Division, Defense Science and Technology Organization, Fishermans Bend, Australia, since 2005.

Shanika Karunasekera received the B.Sc. (engineering) (Hons.) degree in electronics and telecommunication engineering from the University of Moratuwa, Moratuwa, Sri Lanka, in 1990, and the Ph.D. degree in electrical engineering from the University of Cambridge, Cambridge, U.K., in 1995.

She joined the Department of Computing and Information Systems, University of Melbourne, Melbourne, Australia, in 2003, as a Senior Lecturer, where she is currently an Associate Professor.